

# Dispersions of Functionalized Single-Walled Carbon Nanotubes in Strong Acids: Solubility and Rheology

Pradeep K. Rai<sup>1,2</sup>, A. Nicholas G. Parra-Vasquez<sup>1,2</sup>, Jayanta Chattopadhyay<sup>1,3</sup>,  
Robert A. Pinnick<sup>1,2</sup>, Feng Liang<sup>1,3</sup>, Anil K. Sadana<sup>1,3</sup>, Robert H. Hauge<sup>1,3</sup>,  
W. Edward Billups<sup>1,3</sup>, and Matteo Pasquali<sup>1,2,3,\*</sup>

<sup>1</sup>Carbon Nanotechnology Laboratory, Smalley Institute for Nanoscale Science and Technology,

<sup>2</sup>Department of Chemical and Biomolecular Engineering, MS-362, and

<sup>3</sup>Department of Chemistry, MS-60, Rice University, Houston, Texas 77005, USA

The manipulation and processing of single-wall carbon nanotubes (SWNTs) is limited by their poor solubility in most common solvents. Covalent sidewall functionalization of SWNTs provides an excellent route to improve their solubility. Here we have studied the relationship between sidewall functionalization and phase behavior of solutions of functionalized SWNTs (*f*-SWNTs) in strong acids. We use centrifugation in conjunction with UV-Vis-NIR spectroscopy to quantify the solubility of *f*-SWNTs in strong acids. We image the dispersions of functionalized tubes by polarized light microscopy. We find that adding butyl groups increases marginally the solubility of SWNTs in 102% sulfuric acid in the isotropic phase; adding 9-nonadecyne groups roughly doubles the solubility of SWNTs. Viscosity measurements in dilute solutions are sensitive to de-bundling. We compare the viscosity-concentration dependence of dilute pristine and *f*-SWNTs to assess whether and how functionalization promotes de-bundling and stabilizes the tubes. The phase behavior and rheology of these *f*-SWNTs parallels with that of pristine SWNTs; 9-nonadecylated SWNTs have higher solubility and should be easier to process.

**Keywords:** Functionalized Carbon Nanotubes, Solubility, Rheology, Percolation.

## 1. INTRODUCTION

Single-walled carbon nanotubes (SWNTs) hold great potential as ultimate building blocks for high performance materials because of exceptional modulus and strength, low density, and excellent electrical/thermal conductivity.<sup>1–3</sup> A very broad range of applications will be enabled if these exceptional properties of SWNTs can be realized at the macroscopic scale (e.g., in fibers, films, sheets, etc.). The major roadblock in realizing the full potential of SWNTs in macroscopic materials is the difficulty to process them in the liquid state to form fibers and films. As-produced, SWNTs align and pack into ropes<sup>4</sup> due to strong van der Waals forces. Ropes aggregate into tangled networks of poor mechanical and electrical properties.<sup>5</sup> Solubilizing or dispersing SWNTs into solvents has proven very difficult as these strongly held ropes are not easily broken up into individual tubes by either temperature or by solvents.

Various routes for dispersing SWNTs in liquids have been attempted, including searching for solvents for

pristine tubes<sup>6–7</sup> and non-covalent modification of SWNTs by wrapping SWNTs by surfactants<sup>8</sup> or polymers.<sup>9–11</sup> These methods failed to achieve significant solubility. With the aid of surfactants or DNA, SWNTs have been dispersed at low concentration (tens of parts per million as individuals<sup>12</sup> and up to ~1 vol.% as thin bundles).<sup>13</sup> Surfactant-stabilized dispersions, however, must be achieved through sonication, which may damage SWNTs.<sup>14</sup> Recently, strong acids (e.g., fuming sulfuric and chlorosulfonic acids) have been shown to be effective solvents for SWNTs.<sup>15–16</sup> Strong acids do not damage SWNT sidewalls.<sup>15–17</sup> In such acids, SWNTs form dilute isotropic solutions at low concentration (hundreds of ppm); at higher concentrations (above ~8% wt) SWNTs form liquid-crystalline dopes that can be spun into well ordered fibers.<sup>15,18</sup> Despite this important technological achievement, phase behavior studies of SWNTs in superacids reveal that the most common superacid (102% H<sub>2</sub>SO<sub>4</sub> containing 2 wt% excess SO<sub>3</sub>) is not a good solvent (in the Flory sense)<sup>19</sup> for SWNTs.<sup>20–21</sup>

The processability of SWNTs may be improved by functionalizing the sidewalls of SWNTs with other molecules;

\*Author to whom correspondence should be addressed.

yet, this should be done in a careful fashion, to add desirable characteristics without losing the exceptional material (especially electronic) properties of the pristine SWNTs. Perfectly packed arrays of aligned SWNTs may lack shear resistance because the SWNTs interact through central forces and may slip past each other in tension. Recent theoretical work predicts that adding cap-bonding, crosslinks, or functional groups can overcome this problem and boost shear resistance.<sup>22</sup> Functional groups provide a new control “knob” to reduce lateral attraction in overcoming bundling (roping) while at the same time raising the resistance to longitudinal glide in the target-material. The presence of functional groups on the sidewalls of SWNTs provides three kinds of control: (1) Type of the functional group, (2) Length of the functional group, and (3) Density of functional group on the sidewalls of SWNTs.

Recently, functionalized carbon nanotubes have been the subject of vigorous research as functionalization permits easy manipulation for use in diverse technological fields. An excellent review of the latest progress in functionalization approaches, properties, characterization and prospect of functionalized carbon nanotubes can be found in Xiao et al.<sup>23</sup> and references therein. The first covalent modification of single-walled carbon nanotubes to create high-resolution, chemically sensitive probe microscopy tips was reported by Wong et al.<sup>24</sup> Depending on the added sidewall group, carbon nanotubes functionalized by lipophilic or hydrophilic dendra can be stabilized in common organic solvents, such as hexane and chloroform, and water to form colored homogeneous solutions.<sup>25</sup> Carbon nanotubes functionalized with electronic conducting polymers can be used in electronic devices such as supercapacitors.<sup>26</sup> The state-of-the-art research results demonstrate that carbon nanotube/polymer composites have many promising applications to be developed and exploited. Carbon nanotubes modified by conjugated luminescent polymers can form carbon nanotube/polymer composites, which have strong luminescence, and these photo-excited composites may be promising as electron acceptors and optoexcited devices.<sup>26</sup> Lin and coworkers<sup>27</sup> show that poly(vinyl alcohol) functionalized carbon nanotubes are soluble in highly polar solvents such as DMSO and water. The functionalization of carbon nanotubes by the matrix polymer is an effective way of compatibilizing nanotubes with the matrix for high-quality polymeric carbon nanocomposite materials.<sup>27</sup> The improvement of electrical, thermal, and mechanical properties of polymer carbon nanotubes composites through chemical functionalization is widely reported.<sup>28–34</sup> For example, even at loadings as low as 1%, the *f*-MWNT/PMMA composite shows much higher storage modulus and tensile strength than comparable existing composites.<sup>35</sup> Functionalized carbon nanotubes also have huge potential for biological applications. Hu and coworkers<sup>36</sup> synthesized and used polyethyleneimine functionalized single-walled carbon nanotubes as a substrate for neuronal growth and found that it promotes neurite

outgrowth and branching. The possibility of incorporating functionalized carbon nanotubes into cells and the biological milieu offers numerous advantages for potential applications in biology and pharmacology.<sup>37</sup>

Several strategies exist to covalently functionalize SWNTs, such as defect site creation and functionalization from the defects, creating carboxylic acids on the endcaps of carbon nanotubes and subsequent derivatization from the acids, and covalent sidewall functionalization.<sup>38–39</sup> Covalently sidewall modified SWNTs dissolve without sonication,<sup>38–44</sup> but their electronic properties are altered, although frequently these properties can be restored by removing the functional groups after processing by controlled heating.<sup>42</sup> Covalent sidewall functionalization of SWNTs provides an easily scalable way to solubilize nanotubes in common organic solvents like water, chloroform, methanol, and DMF.<sup>42–44</sup> This paper focuses on covalent sidewall functionalized SWNTs (*f*-SWNTs) as it provides the best control over extent of SWNT derivatization and this method is particularly promising for large-scale syntheses.<sup>39</sup>

Here we investigate how covalent sidewall functionalization affects phase behavior and rheology of *f*-SWNTs in sulfuric acid. First, we examine the dispersion quality of *f*-SWNTs in sulfuric through polarizing optical microscopy. This screens the most promising functional groups for easy processing. Next, we determine the solubility of the most promising *f*-SWNTs in superacids and quantify the effect of functional groups. Finally, we report the rheology of these dispersions and relate it to that of sticky bundles of rods.

## 2. EXPERIMENTAL DETAILS

The SWNTs used in this study were produced from the high pressure carbon monoxide (HiPco, batch HPR 120.4) process<sup>4</sup> at Rice University and purified according to literature methods.<sup>45</sup> Purified SWNTs contained less than 5 wt% iron and amorphous carbon impurities. SWNTs were functionalized via reductive alkylation using lithium and alkyl halides in liquid ammonia.<sup>42</sup> In this process, lithium donates its valence electron in liquid ammonia. A part of ammonia solvates the free electron and other part forms a ligand with lithium ion. Ligated lithium intercalates between SWNTs and debundles them. Addition of the alkyl halide leads to the formation of halide anion and the alkyl radical. Radicals readily attach covalently to the debundled nanotubes sidewalls forming individual *f*-SWNTs. Amount of functional group attached to the SWNTs in *f*-SWNTs was determined by TGA. Butylated SWNTs had 20% by mass of butyl group, while 9-nonadecynated SWNTs had 70% by mass of 9-nonadecyne.

102% H<sub>2</sub>SO<sub>4</sub> was used as a solvent; although chlorosulfonic acid is a better solvent, fuming sulfuric at low

$\text{SO}_3$  concentration is easier to handle, it dissolves 10–100 ppm of SWNTs in the isotropic phase,<sup>20</sup> and yields the liquid crystalline phase at high concentration of SWNTs.<sup>15</sup> ACS-certified oleum ( $\sim 20$  wt% excess  $\text{SO}_3$ , density  $1925 \text{ kg/m}^3$ ) was used as received from Sigma Aldrich. 102% sulfuric acid (2 wt% excess  $\text{SO}_3$ , viscosity  $24 \text{ mPa}\cdot\text{s}$  and density  $1880 \text{ kg/m}^3$  at room temperature) was prepared by mixing the oleum with 96% sulfuric acid in the ratio 1.1 ml of oleum/ml of  $\text{H}_2\text{SO}_4$ . The 2% excess  $\text{SO}_3$  ensures that the dispersions are protected against potential uptake of trace amounts of moisture from the environment. The  $\text{SO}_3$  content of the nominal 102% sulfuric acid and oleum was checked by standard titration;<sup>46</sup> the measured  $\text{SO}_3$  content was found to be within 1% of the nominal value. Dispersions of pristine and *f*-SWNTs were prepared by gentle mixing with a magnetic stir bar (no sonication) for a minimum of 72 hours at room temperature in an anhydrous environment (a glovebox with a dewpoint of  $-50^\circ\text{C}$ ) to prevent moisture ingress.

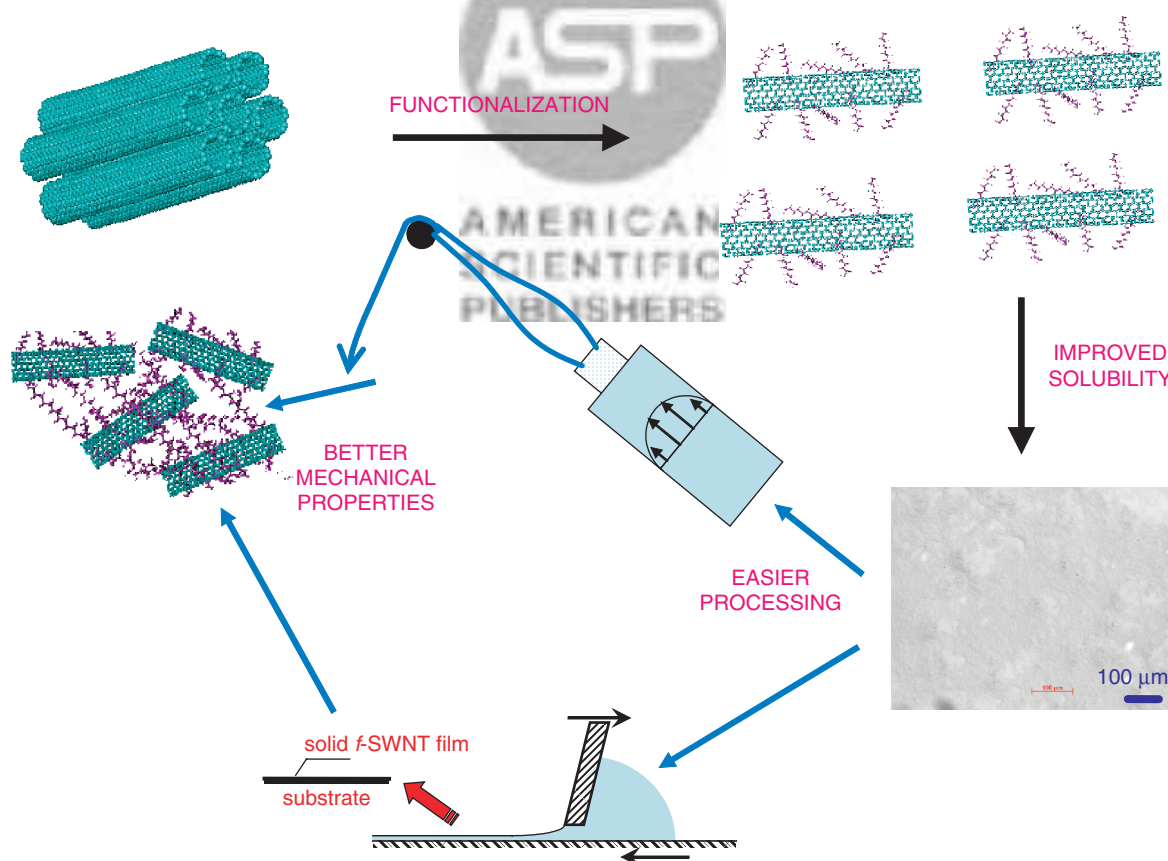
Optical microscopy was performed on a Zeiss Axio-plan optical microscope using flame-dried glass slides and coverslips assembled in the glovebox and sealed with foil tape. Centrifugation experiments were performed on a Fisher Centrifugal Model 225 Benchtop centrifuge at 5100 rpm. UV-Vis-nIR absorbance spectra were measured on a Shimadzu UV-3101PC spectrometer in 1 mm pathlength

Starna cells with teflon closures. Rheological measurements were made on ARES strain-controlled rotational rheometer (Rheometrics Scientific, now TA Instruments, New Castle, DE). The testing fixture was large Couette (Concentric cylinders, internal and external diameters 32 and 34 mm) made of Hastelloy C. An anhydrous environment was maintained during loading and testing of all samples by continuous flow of argon into a custom-made environmental control chamber enclosing the fixture. To provide additional protection against moisture ingress, the sample surface was covered with an inert low viscosity fluid, Fluorinert FC-77 (3M Corp., St. Paul, MN).

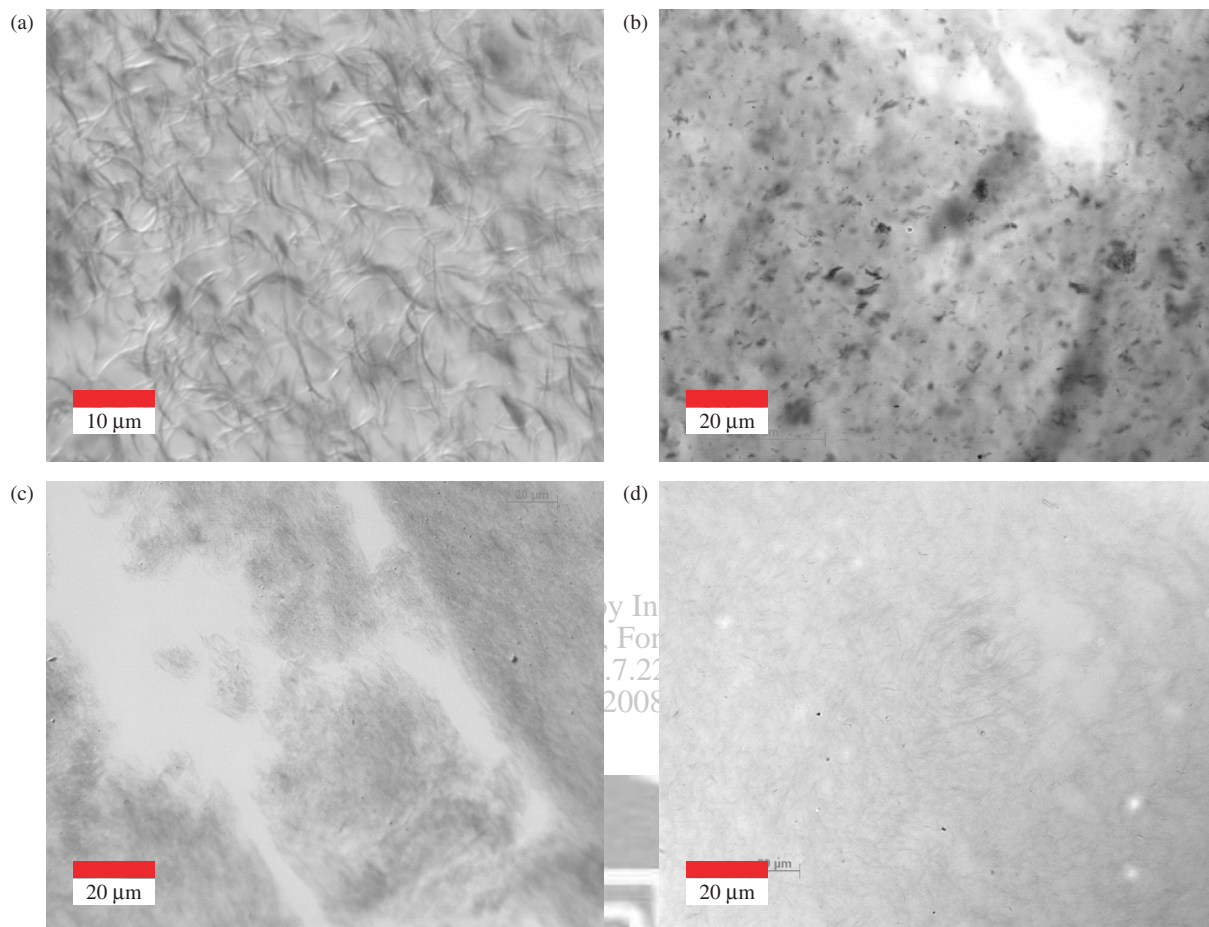
### 3. RESULTS AND DISCUSSION

Figure 1 shows a cartoon of how functionalization can facilitate processing of nanotube dispersions. Functional groups provide steric stabilization of *f*-SWNTs, which lowers their propensity to aggregate into tightly-packed bundles. Stable *f*-SWNT dispersions can be processed easily with conventional scalable methods (like liquid coating or solution spinning) and this should lead to final products with more controlled microstructure and hence better properties.

For a comparative study, the same solvent was used to disperse both pristine and functionalized SWNTs. Figure 2



**Fig. 1.** Schematic envisioned scalable process for making *f*-SWNT materials (e.g., coatings and fibers).



**Fig. 2.** Microscope image of 0.15 wt% dispersion of (a) pristine SWNTs, (b) anilinated SWNTs, (c) butylated SWNTs, and (d) 9-nonadecynated SWNTs in 102%  $\text{H}_2\text{SO}_4$ . Butylated and 9-nonadecynated SWNTs have improved solubility in 102%  $\text{H}_2\text{SO}_4$ .

shows the microscopy images of 0.15 wt% dispersions of pristine and functionalized SWNTs in 102%  $\text{H}_2\text{SO}_4$ . The first image is that of pristine SWNTs. At this concentration, SWNTs are in the biphasic regime, i.e., an isotropic phase in equilibrium with an anisotropic liquid crystalline one.<sup>15</sup> In the liquid crystalline phase, SWNTs are self-assembled into seemingly endless strands termed spaghetti. The second image is that of aniline functionalized SWNTs. Anilinated SWNTs do not disperse in 102%  $\text{H}_2\text{SO}_4$ , as chunks of undissolved SWNTs are clearly visible. The third image is that of butylated SWNTs in the same acid. They are well dispersed at 0.15 wt% concentration and there are no large aggregates: the *f*-SWNTs form tenuous flocs. The last microscopic image is that of 9-nonadecynated SWNTs in 102%  $\text{H}_2\text{SO}_4$  at 0.15 wt%. They are well dispersed in even fainter flocs. Remarkably, at 0.15 wt% concentration in 102% sulfuric acid, unlike pristine SWNTs, butylated and 9-nonadecynated SWNTs do not show any birefringent structure. This is sharply different from the structure of pristine SWNTs in the same acid at same concentration. Owing to their better dispersibility, butylated and 9-nonadecynated SWNTs were chosen for further studies. Other functional groups (including phenyl,

acetonitrile, hexanamide, methyl-PEG, etc.) were considered, but gave similar or worse behavior than anilinated SWNTs.

Solubility measurements of *f*-SWNTs were made by centrifugation in conjunction with UV-Vis-nIR absorbance.<sup>20</sup> Centrifugation of concentrated dispersions (1500 ppm) of *f*-SWNTs for 12 or more hours (during which equilibrium is reached) resulted in a clear phase separation where the dilute phase is supernatant. The concentration of the *f*-SWNTs in the supernatant was determined by diluting the supernatant further with a known amount of acid and then measuring its UV-Vis-nIR absorbance. In all cases, the isotropic phase at the top is optically uniform and structureless when observed under optical microscope. The concentration of SWNTs or *f*-SWNTs in the supernatant phase is its true solubility or isotropic-biphasic transition concentration. Unlike pristine SWNTs,<sup>20</sup> the bottom phase of the *f*-SWNTs shows no birefringence. Figure 3 compares the solubility (concentration of supernatant) of pristine SWNTs and *f*-SWNTs. The isotropic-biphasic transition of pristine SWNTs from HiPco batch 120.4 in 102% sulfuric acid occurs at about 20 ppm.<sup>47</sup> The solubility of butylated SWNTs [from same HiPco batch] is



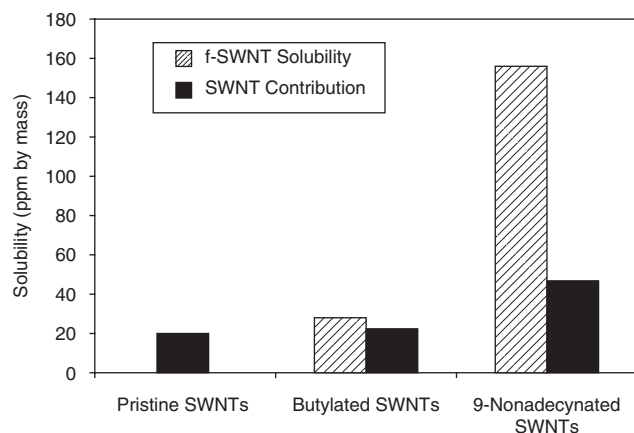
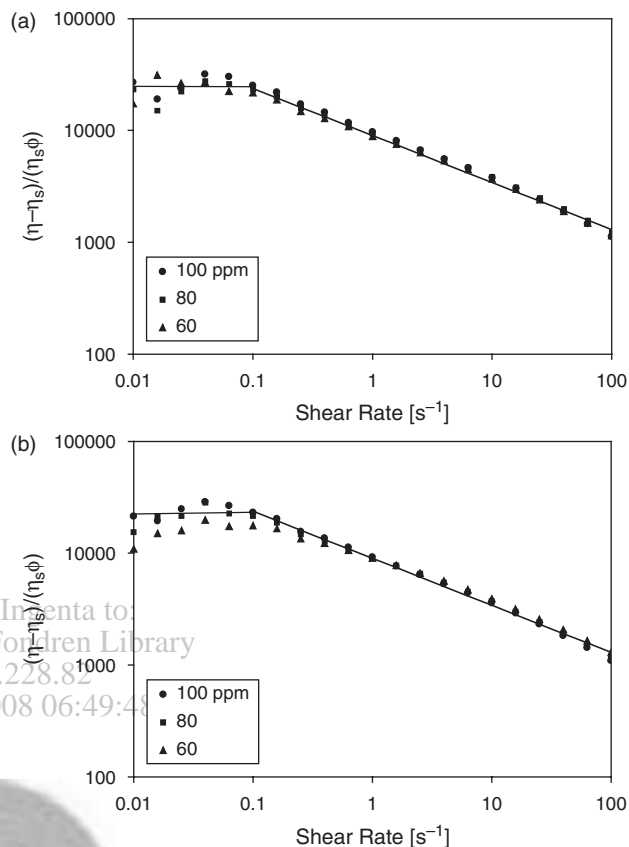


**Fig. 3.** Solubility of pristine functionalized nanotubes showing both total solubility of SWNT + functional group (shaded bars) and the contribution of SWNTs (black bars). The SWNTs contribution to solubility is higher than the solubility of pristine SWNTs in both functionalized samples.

28 ppm; that of 9-nonadecynated SWNTs is 156 ppm. Because *f*-SWNTs have two components (pristine tubes and functional groups), the contribution of SWNTs to the solubility is also shown in the same plot (black bars).

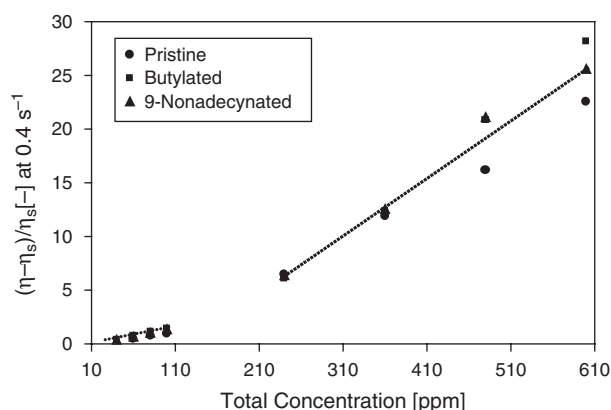
Figure 4 shows the reduced viscosity,  $(\eta - \eta_s)/(\eta_s \phi)$ , versus shear rate for butylated SWNTs and 9-nonadecynated SWNTs in 102%  $H_2SO_4$  at low concentrations. In both the cases, the overlap of reduced viscosity is generally quite good at high shear rates (above  $0.1 \text{ s}^{-1}$ ) for all three concentrations studied, but the overlap of reduced viscosity of the 60 ppm dispersion with that of 100 ppm dispersion is not very good at low shear. According to the centrifugation data, at this concentration the butylated SWNT suspension should have some flocs; however, according to microscopy, such flocs may be so tenuous that they break upon minimal shearing. The rheological data is not sufficiently clean at the low shear rates to determine whether the dispersions are dilute. The zero-shear viscosity of these dispersions is difficult to determine because of limitations of the rheometer's torque transducer at low shear rate. The reduced viscosities of the butylated SWNTs and 9-nonadecynated SWNTs are close at each shear rate; this suggests that the friction coefficient between rod and fluid (which controls the relaxation time) should be comparable in the two cases. Why it should be so is not clear, as nona-decynated groups are considerably larger than butyl ones and therefore should yield a higher friction coefficient. More experiments (including structural information) are needed before drawing conclusions on the dependence of zero-shear viscosity and relaxation time on these functional groups.

Figure 5 summarizes the shear rheology data at concentrations below 600 ppm. On ordinate is relative viscosity,  $(\eta - \eta_s)/\eta_s$ , of the suspensions at  $0.4 \text{ s}^{-1}$ , (all measurements are above the sensitivity of the torque transducer), and abscissa is total concentration in ppm by weight.



**Fig. 4.** Low concentration rheology of functionalized nanotubes (a) butylated SWNTs and (b) 9-nonadecynated SWNTs in 102%  $H_2SO_4$  showing good overlap of reduced viscosity for each of them separately at these concentrations.

At concentration above  $\sim 300$  ppm the dispersions of pristine and *f*-SWNTs are shear thinning at all shear rates (see Fig. 6) above the sensitivity of the torque transducer. There seem to be two concentration regimes: below 200 ppm, viscosity is roughly linear in concentration; above 200 ppm, the dependence seems still linear, but with a steeper slope.



**Fig. 5.** Comparison of relative shear viscosity of pristine and functionalized SWNTs in 102%  $H_2SO_4$  at  $0.4 \text{ s}^{-1}$ . The behaviors of pristine and *f*-SWNTs are similar.

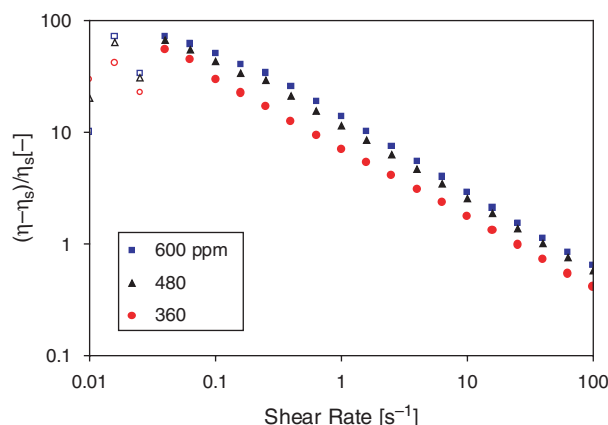


**Fig. 6.** Relative viscosity of 9-nonadecynated SWNTs in 102%  $\text{H}_2\text{SO}_4$  at higher concentrations. The solutions shear thin strongly at all three concentrations at shear rates above  $0.04 \text{ s}^{-1}$ . Below this shear rate (open symbols), the torque is lower than the instrument's sensitivity.

The viscous or loss moduli  $G''$  of a Brownian solution or suspension of perfectly rigid rods have two contributions: one arising from the dissipation by solvent and the other one arising from the dissipation by the movement of rods. The rigid rod contribution is predicted to vary linearly with both concentration and frequency at low frequency. Therefore, the rescaled loss moduli  $(G'' - \eta_s \omega) / \phi$  should scale linearly with frequency at low concentration. Figure 7 shows the rescaled loss moduli of dispersions of 9-noddecynated SWNTs in 102% sulfuric acid. Indeed, at low frequency the rescaled moduli scale roughly linearly with frequency for dilute dispersions (less than 100 ppm in concentration). The same result also holds for pristine SWNTs and butylated SWNTs in 102%  $\text{H}_2\text{SO}_4$ .

Figure 8 shows the linear viscoelastic data of the dispersions of pristine and functionalized SWNTs at 600 ppm concentration. The frequency dependence of elastic and loss moduli is roughly the same for all three dispersions. At low frequency, the dispersions are predominantly elastic

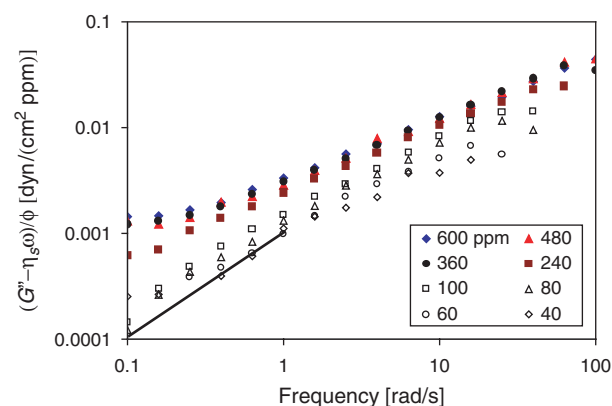


**Fig. 7.** Rescaled loss moduli  $(G'' - \eta_s \omega) / \phi$  of dispersions of 9-nonadecynated SWNTs in 102%  $\text{H}_2\text{SO}_4$ . A slope of 1 is observed here at low frequency in low concentration dispersions (open symbols), as predicted for dilute dispersions of Brownian rods.

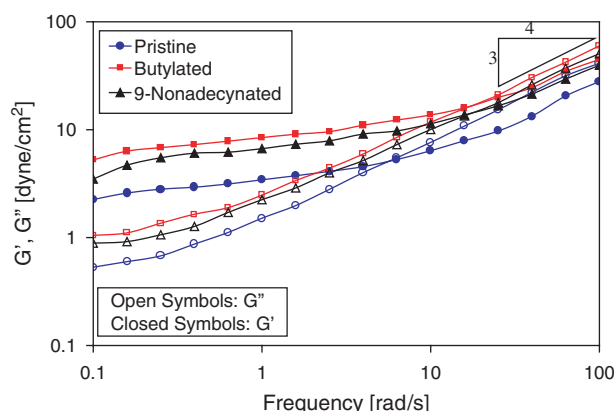


**Fig. 8.** Elastic modulus,  $G'$  (closed symbols) and loss modulus,  $G''$  (open symbols) of 600 ppm dispersions of pristine and functionalized SWNTs at 1% strain.

and  $G'$  flattens out to a constant value. At any concentration, both the elastic and the loss moduli are higher in functionalized tubes than in pristine tubes. The crossover frequency is roughly the same for both butylated and 9-nonadecynated SWNTs; it is lower in pristine SWNTs. At high frequency both  $G'$  and  $G''$  scale to frequency raised to three-fourths in all samples.

SWNT suspensions form viscoelastic solids above a characteristic volume fraction, and this transition can be interpreted as rigidity percolation. SWNTs in suspension form interconnected networks and suspension elasticity originates from interactions between SWNTs rather than from the stiffness or stretching of individual SWNTs.<sup>49</sup> The  $\omega^{3/4}$  scaling for  $G^*$  at high frequencies has been previously reported for semidilute F-actin solutions<sup>50</sup> and concentrated isotropic solutions of semiflexible polymers,<sup>51</sup> but for an entirely different physical reason. For semiflexible polymers, this is due to the fact that, at high frequencies, the wavelength of any excitation is shorter than the average entanglement of the filaments, and  $G^*(\omega)$  reflects directly the single filament response. For dispersions of rigid rods, however, it is the response of a network of rods rather than the response of a single rod. The suspensions switch from viscous to elastic like behavior at  $\sim 360$  ppm for pristine SWNTs and at  $\sim 240$  ppm for the two *f*-SWNTs dispersions; however, a clear plateau in elastic modulus appears only close to 600 ppm in concentration suggesting the onset of percolation of nanotubes.

## 4. CONCLUSIONS

From many potential functional groups, two sidewall groups have been identified for improving the behavior of SWNTs in scalable liquid-based processing like coating and fiber spinning. Butylated and 9-nonadecynated SWNTs have good dispersibility and solubility in 102% sulfuric acid. At low concentrations, *f*-SWNTs behave as Brownian rods and dissolve as individuals in 102%  $\text{H}_2\text{SO}_4$ .

The phase behavior and rheology of these *f*-SWNTs parallels with that of pristine SWNTs; however, they self-assemble into loose flocs rather than liquid crystalline strands. The nonadecynated SWNTs form flocs at higher concentration; thus, they are likely to yield easier processing. At higher concentration, the storage modulus dominates at low frequencies and attains a plateau independent of frequency reflecting the solidlike behavior resulting from the resistance of the percolation of rods to mechanical rotation. Solubility measurements and linear viscoelastic measurements on dispersions of *f*-SWNTs follow a behavior previously reported in literature for surfactant-stabilized SWNTs. Future work will address the effect of functionalization on material properties of macroscopic fibers and sheets or films—e.g., modulus, strength, electrical and thermal conductivity, and capacitance.

**Acknowledgments:** We acknowledge the help of Virginia Davis, Carter Kittrell, Wade Adams, Wen-Fang Hwang, Howard Smith, and James Tour. Financial support was provided by the Advanced Technology Program of the state of Texas under Grant 003604-0113-2003, by the DURINT initiative of the Office of Naval Research under Grant N00014-01-1-0789 by the Robert A. Welch Foundation under Grant C-0490 and by the National Science Foundation under Grant CHE-0011486.

## References and Notes

1. R. H. Baughman, A. A. Zakhidov, and W. A. de Heer, *Science* 297, 787 (2002).
2. J. Hone, M. C. Llaguno, N. M. Nemes, A. T. Johnson, J. E. Fischer, D. A. Walters, M. J. Casavant, J. Schmidt, and R. E. Smalley, *Appl. Phys. Lett.* 77, 666 (2000).
3. J. Hone, M. Whitney, C. Piskoti, and A. Zettl, *Phys. Rev. B* 59, R2514 (1999).
4. M. J. Bronikowski, P. A. Willis, D. T. Colbert, K. A. Smith, and R. E. Smalley, *J. Vac. Sci. Technol. A: Vac. Surf. Films* 19, 1800 (2001).
5. B. Vigolo, A. Penicaud, C. Coulon, C. Sauder, R. Pailler, C. Journet, P. Bernier, and P. Poulin, *Science* 290, 1331 (2000).
6. K. D. Ausman, R. Piner, O. Lourie, R. S. Ruoff, and M. J. Korobov, *Phys. Chem. B* 104, 8911 (2000).
7. Y. Sun, S. R. Wilson, and D. I. Schuster, *J. Am. Chem. Soc.* 123, 5348 (2001).
8. H. Wang, W. Zhou, D. L. Ho, K. I. Winey, J. E. Fischer, C. J. Glinka, and E. K. Hobbie, *Nano Lett.* 4, 1789 (2004).
9. M. Zheng, A. Jagota, E. D. Semke, B. A. Diner, R. S. Mclean, S. R. Lustig, R. E. Richardson, and N. G. Tassi, *Nat. Mater.* 2, 338 (2003).
10. M. Zheng, A. Jagota, M. S. Strano, A. P. Santos, P. Barone, S. G. Chou, B. A. Diner, M. S. Dresselhaus, R. S. Mclean, G. B. Onoa, G. G. Samsonidze, E. D. Semke, M. Usrey, and D. J. Walls, *Science* 302, 1545 (2003).
11. M. S. Strano, M. Zheng, A. Jagota, G. B. Onoa, D. A. Heller, P. W. Barone, and M. L. Usrey, *Nano Lett.* 4, 543 (2004).
12. V. C. Moore, M. S. Strano, E. H. Haroz, R. H. Hauge, R. E. Smalley, H. K. Schmidt, and Y. Talmon, *Nano Lett.* 3, 1379 (2003).
13. M. F. Islam, E. Rojas, D. M. Bergey, A. T. Johnson, and A. G. Yodh, *Nano Lett.* 3, 269 (2003).
14. K. B. Shelimov, R. O. Esenaliev, A. G. Rinzier, C. B. Huffman, and R. E. Smalley, *Chem. Phys. Lett.* 282, 429 (1988).
15. V. A. Davis, L. M. Ericson, A. N. G. Parra-Vasquez, H. Fan, Y. Wang, V. Prieto, J. A. Longoria, S. Ramesh, R. K. Saini, C. Kittrell, W. E. Billups, W. W. Adams, R. H. Hauge, R. E. Smalley, and M. Pasquali, *Macromolecules* 37, 154 (2004).
16. S. Ramesh, L. M. Ericson, V. A. Davis, R. K. Saini, C. Kittrell, M. Pasquali, W. E. Billups, W. W. Adams, R. H. Hauge, and R. E. Smalley, *J. Phys. Chem. B* 108, 8794 (2004).
17. C. Engtrakul, M. F. Davis, T. Gennett, A. C. Dillon, K. M. Jones, and M. J. Heben, *J. Am. Chem. Soc.* 127, 17548 (2005).
18. L. M. Ericson, H. Fan, H. Peng, V. A. Davis, W. Zhou, J. Sulpizio, Y. Wang, R. Booker, J. Vavro, C. Guthy, A. N. G. Parra-Vasquez, M. J. Kim, S. Ramesh, R. K. Saini, C. Kittrell, G. Lavin, H. K. Schmidt, W. W. Adams, W. E. Billups, M. Pasquali, W.-F. Hwang, R. H. Hauge, J. E. Fischer, and R. E. Smalley, *Science* 305, 1447 (2004).
19. P. J. Flory, *Principles of Polymer Chemistry*, Cornell University Press, Ithaca (1953).
20. P. K. Rai, R. A. Pinnick, A. N. G. Parra-Vasquez, V. A. Davis, H. K. Schmidt, R. H. Hauge, R. E. Smalley, and M. Pasquali, *J. Am. Chem. Soc.* 128, 591 (2006).
21. V. A. Davis, P. K. Rai, V. Prieto, A. N. G. Parra-Vasquez, W. Zhou, H. Fan, R. H. Hauge, J. E. Fischer, R. E. Smalley, and Matteo Pasquali, "Effects of Solvent Quality on SWNT Liquid Crystal Phase Behavior and Morphology of Solution Spun Fibers," In preparation.
22. Y. Zhao, B. I. Yakobson, and R. E. Smalley, *Phys. Rev. Lett.* 88, 185501 (2002).
23. S. F. Xiao, Z. H. Wang, and G. A. Luo, *Chinese J. Anal. Chem.* 33, 261 (2005).
24. S. S. Wong, A. T. Woolley, E. Joselevich, C. L. Cheung, and C. M. Lieber, *J. Am. Chem. Soc.* 120, 8557 (1998).
25. Y. P. Sun, W. J. Huang, Y. Lin, K. F. Fu, A. N. Kitaygorodskiy, L. A. Riddle, Y. J. Yu, and D. L. Carroll, *Chem. Mater.* 13, 2864 (2001).
26. L. X. Li, F. Li, Z. Ying, Q. H. Yang, and H. M. Cheng, *New Carbon Mater.* 18, 69 (2003).
27. Y. Lin, B. Zhou, K. A. S. Fernando, P. Liu, L. F. Allard, and Y. P. Sun, *Macromolecules* 36, 7199 (2003).
28. R. Sen, B. Zhao, D. Perea, M. E. Itkis, H. Hu, J. Love, E. Bekyarova, and R. C. Haddon, *Nano Lett.* 4, 459 (2004).
29. L. W. Qu, Y. Lin, D. E. Hill, B. Zhou, W. Wang, X. F. Sun, A. N. Kitaygorodskiy, M. Suarez, J. W. Connell, L. F. Allard, and Y. P. Sun, *Macromolecules* 37, 6055 (2004).
30. B. Philip, J. N. Xie, J. K. Abraham, and V. K. Varadan, *Polym. Bull.* 53, 127 (2005).
31. S. Bhattacharyya, C. Sinturel, J. P. Salvetat, and M. L. Saboungi, *Appl. Phys. Lett.* 86, 113104 (2005).
32. S. H. Zhang, N. Y. Zhang, C. Huang, K. L. Ren, and Q. M. Zhang, *Adv. Mater.* 17, 1897 (2005).
33. G. M. Odegard, S. J. V. Frankland, and T. S. Gates, *AIAA J.* 43, 1828 (2005).
34. L. Q. Liu, A. H. Barber, S. Nuriel, and H. D. Wagner, *Adv. Funct. Mater.* 15, 975 (2005).
35. C. Velasco-Santos, A. L. Martinez-Hernandez, F. T. Fisher, R. Ruoff, and V. M. Castano, *Chem. Mater.* 15, 4470 (2003).
36. H. Hu, Y. C. Ni, S. K. Mandal, V. Montana, N. Zhao, R. C. Haddon, and V. Parpura, *J. Phys. Chem. B* 109, 4285 (2005).
37. K. Kostarelos, L. Lacerda, C. D. Partidos, M. Prato, and A. Blanco, *J. Drug Deliv. Sci. Tech.* 15, 41 (2005).
38. C. A. Dyke and J. M. Tour, *Chem.-A Euro. J.* 10, 813 (2004); *J. Phys. Chem. A* 108, 11151 (2004).
39. Y. Ying, R. K. Saini, F. Liang, A. K. Sadana, and W. E. Billups, *Org. Lett.* 5, 1471 (2003).
40. C. A. Dyke, M. P. Stewart, F. Maya, and J. M. Tour, *Synlett* 155 (2004).
41. B. K. Price, J. L. Hudson, and J. M. Tour, *J. Am. Chem. Soc.* 127, 14867 (2005).
42. F. Liang, A. K. Sadana, A. Peera, J. Chattopadhyay, Z. Gu, R. H. Hauge, and W. E. Billups, *Nano Lett.* 4, 1257 (2004).

43. J. Chattopadhyay, A. K. Sadana, F. Liang, J. M. Beach, Y. Xiao, R. H. Hauge, and W. E. Billups, *Org. Lett.* **7**, 4067 (2005).
44. F. Liang, L. B. Alemany, J. M. Beach, and W. E. Billups, *J. Am. Chem. Soc.* **127**, 13941 (2005).
45. I. W. Chiang, B. E. Brinson, A. Y. Huang, P. A. Willis, M. J. Bronikowski, J. L. Margrave, R. E. Smalley, and R. H. Hauge, *J. Phys. Chem. B* **105**, 8297 (2001).
46. Sulfuric Acid, Fuming, Reagent Chemicals, American Chemical Society, Washington, DC (2002), 9th edn., Vol. 645.
47. Because the HiPco reactor conditions are changed from batch to batch, certain properties of SWNT samples change accordingly, e.g., the length<sup>48</sup> and diameter distribution; it is suspected that some reaction condition affect the ratio of metallic to semiconducting tubes. All these factors affect the critical isotropic-biphasic transition of SWNTs in acids.
48. R. L. Carver, H. Q. Peng, A. K. Sadana, P. Nikolaev, S. Arepalli, C. D. Scott, W. E. Billups, R. H. Hauge, and R. E. Smalley, *J. Nanosci. Nanotechnol.* **5**, 1035 (2005).
49. L. A. Hough, M. F. Islam, P. A. Janmey, and Y. G. Yodh, *Phys. Rev. Lett.* **93**, 168102 (2004).
50. T. Gisler and D. A. Weitz, *Phys. Rev. Lett.* **82**, 1606 (1999).
51. D. C. Morse, *Macromolecules* **31**, 7030 (1998).

Received: 23 June 2006. Revised/Accepted: 10 September 2006.

Delivered by Ingenta to:  
Rice University, Fondren Library  
IP : 168.7.228.82  
Tue, 12 Feb 2008 06:49:48

